Angela Bonaccorso
Istituto Nazionale di Fisica Nucleare
SEZIONE DI PISA

CORTONA 2013
XIV CONVEGNO su PROBLEMI di FISICA NUCLEARE TEORICA
29–31 OTTOBRE 2013

Reazioni dirette con fasci radioattivi

Phys. Scr. T152 (2013) 014019 doi:10.1088/0031-8949/2013/T152/014019

Angela Bonaccorso

INFN, Sez. di Pisa

Entering the world of exotic nuclei

http://www.eurisol.org/usergroup/

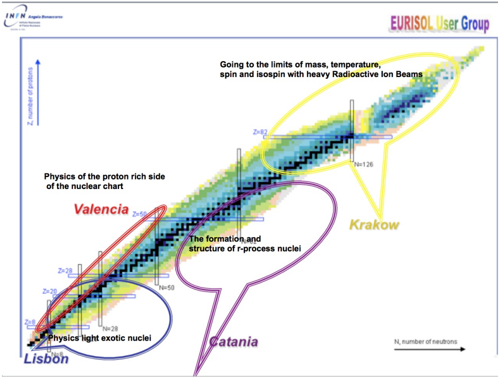

- Exotic nuclei can be found in the crust of neutron's stars.
- Is there a life behind the dripline?
- Extend our understanding of the nuclear force.
- Check the limits of validity of structure models.
- In practice AFA my talk is concerned: try do do spectroscopy in extreme conditions.

Reaction talks to follow in this session

The rôle of Reaction Theory

We have at present very sophisticated structure models and extremely complex experiments with relatively "simple" interpretations for the data.

"Ab initio" models have started to bridge the gap between structure and reaction theory (see Eurisol Lisbon Meeting report on "Physics of Light Exotic Nuclei").

In this panorama, which is the rôle of Reaction Theory and how simple and/or "complicated" does it need to be?

- Understanding the reaction mechanisms.
- Search for the best *observable* to be measured (in view of the reduced intensity of RB).
- Accuracy of methods and numerical implementations.

Plan of the Presentation

Early experiments: halo nuclei

I. Tanihata et al., Phys. Lett. B 160, 380 (1985)

$$\sigma_R = \pi\left(R_{vol} + R_{surf}\right)^2\left(1 - \frac{B_c}{E_{cm}}\right)$$

Kox et al. (1987)

$$\sigma_I = \pi\left[R_I(P) + R_I(T)\right]^2$$

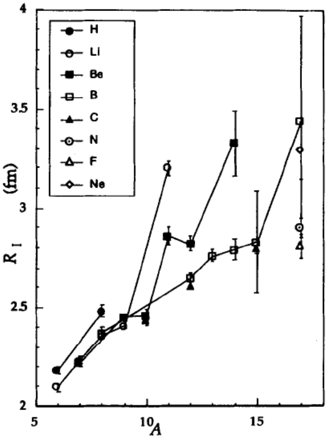

Fig. 2.1 Interaction cross sections of light nuclei determined by 800A MeV reactions.

Early eikonal model

M. S. Hussein & K.W. Mc Voy, NPA445 124(1985)

I. Tanihata, Prog. Part. Nucl. Phys. 35, 505 (1995)

These equations provide a simple way to compare the reaction cross sections at different energies. However, since they are purely empirical formula, one should be careful when applying them to an exotic nucleus because of a possible difference in the surface diffuseness as well as any proton-neutron density difference. When one measures σ_R using a β-unstable nucleus, only r_0 is expected to change.

$$\begin{aligned}\sigma_R &= \int_0^\infty d\mathbf{b}(1 - |S(\mathbf{b})|^2) \\ &= \sigma_{ct} + \sigma_{nt}\end{aligned}$$

decoupling of core and halo,

$$\rho_p = \rho_c + \rho_n$$

where

$$\sigma_{nt} = \int_0^\infty d\mathbf{b}|S_{ct}|^2 P_{b_{up}}$$

if

$$\begin{aligned}|S(\mathbf{b})|^2 &= e^{-[\sigma_{nn}\int ds\rho_p(|b-s|)\rho_t(s)]} \\ &= e^{-[\sigma_{nn}\int ds\rho_c\rho_t]}e^{-[\sigma_{nn}\int ds\rho_n\rho_t]}\end{aligned}$$

$$|S_{nt}|^2 \approx e^{-\sigma_{nn}\int ds\rho_n\rho_t} \approx 1 - \sigma_{nn}\int ds\rho_n\rho_t \approx 1 - P_{b_{up}}$$

$$|S(\mathbf{b})|^2 = |S_{ct}|^2|S_{nt}|^2 = |S_{ct}|^2 - |S_{ct}|^2 P_{b_{up}}$$

Transfer: to bound states vs to continuum states (inclusive reaction)

Kinematics and phase space ++

Single particle state properties (shell model)

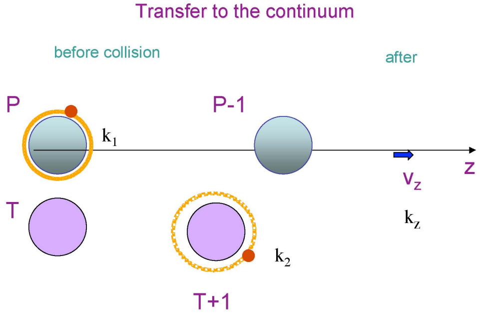

$k_2 - k_1 = k_z$

$\varepsilon_f - \varepsilon_i = mv^2/2$

Removal of a deeply bound n/p while the weakly bound p/n is un-touched *

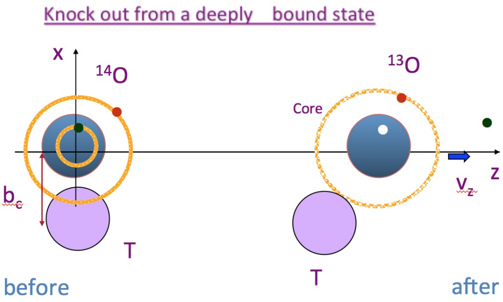

Sketch of coordinates

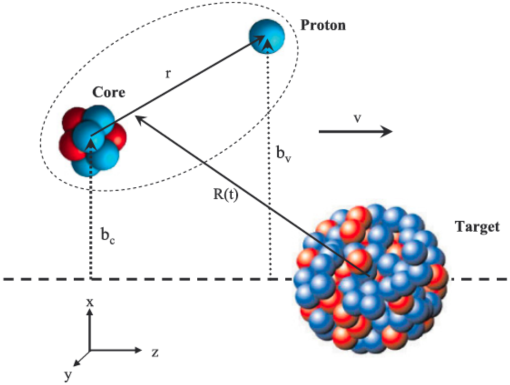

A consistent formalism for normal and exotic nuclei

The core-target movement is treated in a semiclassical way, but neutron-target and/or neutron-core in a full QM treatment.

H. Hasan and D.M. Brink, J Phys G4, 1573 (1978); AB and DM Brink, PRC38, 1776 (1988), PRC43, 299 (1991), PRC44, 1559 (1991). R. A. Broglia and A. Winther, Heavy Ion Reactions (Addison-Wesley, 1991).

$$\frac{d\sigma}{d\xi} = C^2 S \int_0^\infty d\mathbf{b_c} \frac{dP_{-n}(b_c)}{d\xi} P_{ct}(b_c),$$

$$\xi \to \varepsilon_f, k_z, P_{//} \quad also \quad ANC = C^2 S C_i^2$$

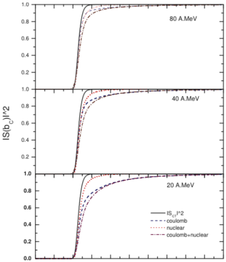

Use of the simple parametrization $P_{ct}(b_c) = |S_{ct}|^2 = e^{(-\ln 2 exp[(R_s - b_c)/a])}$,

$$R_s \approx 1.4(A_p^{1/3} + A_t^{1/3}) fm$$

'strong absorption radius'.

Absolute cross sections $\sigma = \int d\xi \frac{d\sigma}{d\xi}$

Ratios

$$\sigma_{exp}/\sigma_{Theo}$$

have been used to validate spectroscopic factors C^2S (=2j+1, in the IPM) for single particle orbitals from shell model or "ab initio" calculations, when available. This is similar to what has traditionally been done for transfer. However in transfer the core-target interaction is treated almost exactly thanks to optical potentials fitted to the elastic scattering.

C. Barbieri PRL103, 202502 (2009)

The reactions for transfer of a nucleon to or from the initial state $|\Psi_0^A\rangle$ depend on the overlap wave function [8,9]

$$\psi_\alpha^{A\pm1}(\mathbf{r}) = \langle \Psi_\alpha^{A\pm1} | \psi^{(\dagger)}(\mathbf{r}) | \Psi_0^A \rangle, \qquad (1)$$

where α can label either particle or hole states. SFs are identified with the normalization integral of $\psi_\alpha^{A\pm1}(\mathbf{r})$ and give a "measure" of what fraction of the *final* wave function, $|\Psi_\alpha^{A\pm1}\rangle$, can be factorized into a (correlated) core plus an independent particle or hole. Strong deviations from the independent particle model (IPM)—that is, a Slater determinant with fully occupied orbits—signal substantial correlations and imply the onset of nontrivial many-body dynamics. For stable nuclei, a large body of

A. Gade *et al*, PRL. **93** 042501 (2004) ; PRC **77**, 044306 (2008)

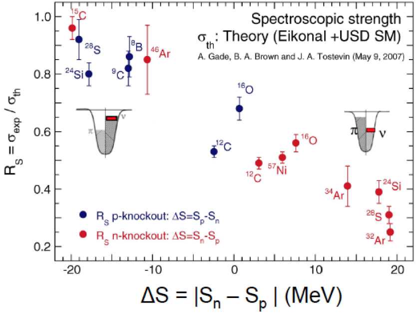

J. Lee *et al*, PRC **83**, 014606 (2011).

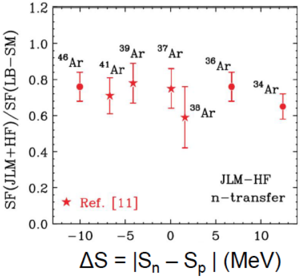

Table : EXAMPLE: Separation energies (MeV) in Oxigen and Carbon

	^{14}O	^{13}O	^{16}C	^{15}C
S_n	23.1	17.0	4.25	1.2
S_p	4.6	1.5	22.56	21.08

A possible (partial) reason: Transfer to the continuum vs eikonal ⊗ ∗

First order time dependent perturbation theory amplitude:

$$A_{fi} = \frac{1}{i\hbar}\int_{-\infty}^{\infty} dt < \phi_f(\mathbf{r})|V(\mathbf{r})|\phi_i(\mathbf{r}-\mathbf{R}(t)) > e^{-i(\omega t - mvz/\hbar)} \qquad (1)$$

$$\omega = \varepsilon_i - \varepsilon_f + \tfrac{1}{2}mv^2 \qquad \mathbf{R}(t) = \mathbf{b_c} + vt$$

$$\frac{dP_{-n}(b_c)}{d\varepsilon_f} = \frac{1}{8\pi^3}\frac{m}{\hbar^2 k_f}\frac{1}{2l_i+1}\Sigma_{m_i}|A_{fi}|^2$$
$$\approx \frac{4\pi}{2k_f^2}\Sigma_{j_f}(2j_f+1)(|1-\bar{S}_{j_f}|^2 + 1 - |\bar{S}_{j_f}|^2)\mathcal{F},$$

This general QM formalism allows for transfer to sp resonances in the target via the optical model $\bar{S}$-matrix and contains the Trojan Horse method

$$\mathcal{F} = (1 + F_{l_f,l_i,j_f,j_i})B_{l_f,l_i} \qquad B_{l_f,l_i} = \frac{1}{4\pi}\left[\frac{k_f}{mv^2}\right]|C_i|^2\frac{e^{-2\eta b_c}}{2\eta b_c}M_{l_f l_i}$$

Kinematics

From Eq.1 by the change of variables $dtdxdydz \to dxdydzdz'$
$e^{-i(\omega t - mvz/\hbar)} \to e^{-ik_1 z'} e^{ik_2 z}$ neutron energies to neutron parallel momenta with respect to core

$$k_1 = \frac{\varepsilon_f - \varepsilon_i - \frac{1}{2} mv^2}{\hbar v};$$

to target

$$k_2 = \frac{\varepsilon_f - \varepsilon_i + \frac{1}{2} mv^2}{\hbar v};$$

to core parallel momentum

$$\begin{aligned} P_{//} &= \sqrt{E_r^2 - M_r^2} = \sqrt{(T_r + M_r)^2 - M_r^2} \\ &= \sqrt{(T_p + \varepsilon_i - \varepsilon_f)^2 + 2M_r(T_p + \varepsilon_i - \varepsilon_f)}, \end{aligned} \tag{2}$$

breakup threshold at $\varepsilon_f = 0$

++**

Eikonal limit

Small neutron scattering angles

$$M_{l_f l_i} \approx P_{l_i}(X_i) P_{l_f}(X_f); \qquad P_{l_f}(X_f) \to J_0(2\eta \mathbf{b_v})$$

large n-t angular momenta

$$\frac{4\pi}{2k_f^2} \Sigma_{j_f}(2j_f + 1) \to \int_0^\infty d\mathbf{b_v}$$

both conditions might not be well satisfied for stripping of deeply bound nucleons unless the core-target scattering is very peripheral. Verify core angular distributions.

$$P_{-n}(\mathbf{b_c}) = \int_0^\infty d\mathbf{b_v}[|1 - \bar{S}(b_v)|^2 + 1 - |\bar{S}(b_v)|^2)] \tilde{\phi}_i(|\mathbf{b_v} - \mathbf{b_c}|, k_1)|^2$$

Notice $k_1 \to -\infty$ not strictly necessary.

Wave functions

Final continuum state:

$$\phi_f(\mathbf{r}) = C_f k \frac{i}{2}(h_{l_f}^{(+)}(kr) - \bar{S}_{l_f} h_{l_f}^{(-)}(kr)) Y_{l_f,m_f}(\Omega_f),$$

$\bar{S}_{l_f}(\varepsilon_f)$ is an optical model n-t (n-core in fragmentation reactions) S-matrix.

or using the potential $V = V_{\rm nt} + V_{\rm eff}$ sum of the neutron-target optical and Coulomb potentials, a distorted wave of the eikonal-type

$$\phi_f(\mathbf{r}, \mathbf{k}) = exp\{i\mathbf{k}\cdot\mathbf{r} + i\chi_{\rm eik}(\mathbf{r}, t)\} \tag{3}$$

the eikonal phase shift is simply

$$\chi_{\rm eik}(\mathbf{r}, t) = \frac{1}{\hbar}\int_t^\infty V(\mathbf{r}, \mathbf{R}(t'))dt'. \tag{4}$$

Divergence in first order Coulomb eikonal is regularized replacing with first order time dependent perturbation theory.

J. Margueron, AB, DM Brink, NPA720 (2003) 337.

Initial state:

$$\phi_i(\mathbf{r}) = -C_i i^l \gamma h_{l_i}^{(1)}(i\gamma r) Y_{l_i,m_i}(\Omega_i).$$

L. Lo Monaco and DM Brink JPG11, 935, 1985; A. Mukhamedzhanov PRC 84, 044616, 2011; I. Thomposon talk at DREB2012 (Pisa).

Origin of kinematical cut-off and deformation effects PRC60(1999) 054604,PRC44(1991) 1559

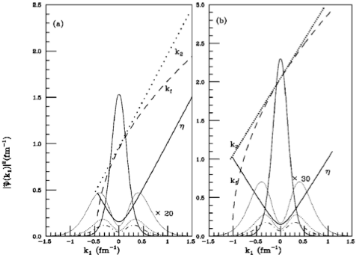

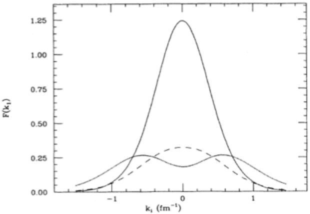

FIG. 11. Initial-state momentum distributions in ^{20}Ne according to Eq. (2.3a). The solid curve is for the $2s_{1/2}$ state, the dashed curve is the for $1p_{1/2}$, while the dotted curve is for the $1d_{5/2}$ state.

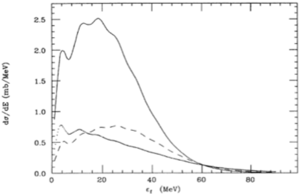

FIG. 7. Calculated total spectrum of the reaction ^{208}Pb(^{20}Ne,^{19}Ne)^{209}Pb at $E_{\mathrm{inc}}=40$ MeV/nucleon. The solid curve is for the $2s_{1/2}$ initial state, the dashed curve is for the $1p_{1/2}$ initial state, while the dotted curve is for the $1d_{5/2}$ initial state.

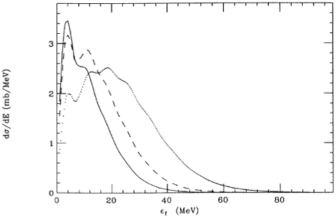

FIG. 8. Calculated total spectrum of the reaction ^{208}Pb(^{20}Ne,^{19}Ne)^{209}Pb for the $2s_{1/2}$ initial state. The solid curve is at $E_{\mathrm{inc}}=25$ MeV/nucleon, the dashed curve is at $E_{\mathrm{inc}}=30$ MeV/nucleon, and the dotted curve is at $E_{\mathrm{inc}}=40$ MeV/nucleon.

(+)

Example of kinematical cut-off effects AB and GF Bertsch, PRC63(2001) 044604; F. Flavigny et al., PRL 108, 252501 (2012).

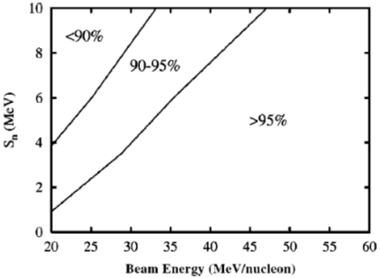

FIG. 1. Ratio of phase space integrals with and without momentum cutoffs, for a d-wave neutron wave function. The effect of the cutoff is to include less than 90%, between 90% and 95%, and more than 95% of the initial momentum distribution as marked on the figure.

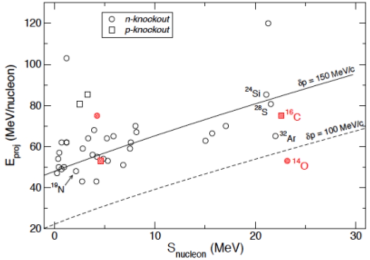

FIG. 3: (Color online) Nucleon-removal experiments from the literature [7, 22, 34] plotted as a function of the energy per nucleon of the projectile and the separation energy of the removed nucleon. The lines correspond to cutoffs appearing at $\delta p = 100$ and 150 MeV/c with respect to the center of the SE distribution. Data from the present experiment are in red.

Example of kinematical cut-off effects AB and GF Bertsch, PRC63(2001) 044604; F. Flavigny et al., PRL 108, 252501 (2012).

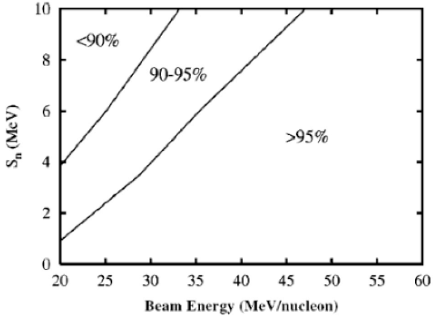

FIG. 1. Ratio of phase space integrals with and without momen-

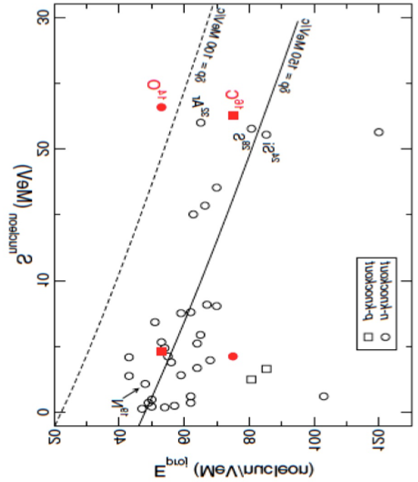

FIG. 3: (Color online) Nucleon-removal experiments from the

Example of kinematical deformation effects

F. Flavigny, A. Obertelli, AB et al., PRL 108, 252501 (2012). **

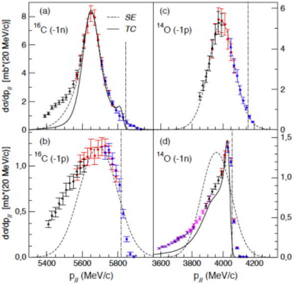

J.Enders et al. PHYSICAL REVIEW C **65** 034318

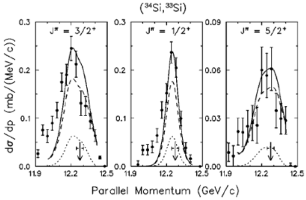

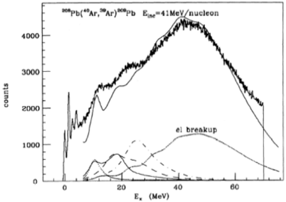

AB et al., PRC49(1994)

Another possible reason? (R. Kumar (eikonal) and G. Salvioni (TC) MSc thesis in progress)

$$\sigma = C^2 S \int_0^\infty d\mathbf{b_c} P_{-n}(b_c)(1 - P_{-p}(b_c))P_{ct}(b_c)$$

$$e^{-P_{-p}} \approx 1 - P_{-p}(b_c)$$

dpp from phase shift, AB, F. Carstoiu, NPA706, (2002)

$$|S_{NN}(b_c)|^2 = e^{-4\delta_I(b_c)} = e^{-4\delta_I^V(b_c)} e^{-4\delta_I^S(b_c)} = |S_{ct}(b_c)|^2 e^{-P_{-p}(b_c)}$$

with

$$\delta_I(b_c) = -\frac{1}{2\hbar v} \int dz (W_V(b_c, z) + W_S(b_c, z))$$

$$-4\delta_I^S(b_c) = \frac{2}{\hbar v}\left[\int_{-\infty}^{+\infty} W_S(b_c, z) dz\right] = \frac{2}{\hbar v}\left[(-\frac{\hbar v}{2})P_{-p}(b_c)\right]$$

typically 10% reduction in the cross sections.

Elastic scattering

A. Di Pietro et al., PRL 105 (2010) 22701

see also PRC67, 044602; NPA803 (2008) 30; PRC85 (2012) 054607; PRC77, 054606; NPA840 (2010)19.

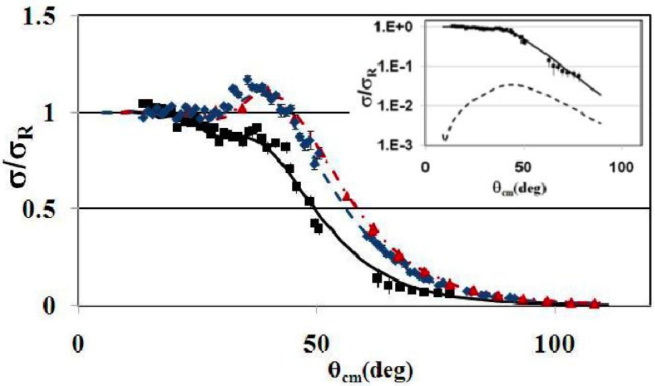

TABLE I: W-S Optical potentials obtained from the fit of the experimental data. The real potential radius parameter is r_0=1.1 fm and the imaginary one is r_i=1.2 fm, where $R_{0,i,si}=r_{0,i,si}(A_p^{1/3}+A_t^{1/3})$. The Coulomb radius parameter is r_C=1.25 fm.

Reaction	V(MeV)	a(fm)	V_i(MeV)	a_i(fm)	V_{si}(MeV)	r_{si}(fm)	a_{si}(fm)	J_V(MeV fm^3)	J_W(MeV fm^3)
^{9}Be+^{64}Zn	126	0.6	17.3	0.75				295	53
^{10}Be+^{64}Zn	86.2	0.7	43.4	0.7				193	124
^{11}Be+^{64}Zn	86.2	0.7	43.4	0.7	0.151	1.3	3.5	193	129

Absolute cross sections, F. Flavigny, A. Obertelli, AB et al., PRL 108, 252501 (2012)

$$\sigma_{exp}/\sigma_{Eik} = 0.25 \qquad \sigma_{exp}/\sigma_{TC} = 0.41$$

TABLE I. Summary of one-nucleon knockout results from ^{14}O at 53 MeV/nucleon and ^{16}C at 75 MeV/nucleon. We show inclusive cross sections σ_{SE} from the sudden and eikonal approach and σ_{TC} from the transfer to the continuum approach and the measured (σ_{exp}) cross sections. Spectroscopic factors C^2S are calculated with the WBT interaction in the *psd* valence space [18].

Beam	Res.	E (MeV)	J^π	σ_{exp} (mb)	C^2S	σ_{SE} (mb)	σ_{TC} (mb)
^{14}O	^{13}N	0.0	$1/2^-$	58(4)	1.55	55	not applicable
^{14}O	^{13}O	0.0	$3/2^-$	14(1)	3.15	54	34
^{16}C	^{15}B	0.0	$3/2^-$	18(2)	2.95	50	not applicable
		1.33	$(5/2^-)$	1.3(2)	...	...	...
		2.73	$(7/2^-)$	0.8(1)	...	...	...
^{16}C	^{15}C	0.0	$1/2^+$	36(5)	0.89	60	59
		0.74	$5/2^+$	46(6)	0.90	30	31
		total		81(7)		90	90

Transfer of a deeply bound n/p while the weakly bound p/n is un-touched

F. Flavigny et al. Self consistent Green function (SCGF) form factors (C. Barbieri)

PRL **110,** 122503 (2013) PHYSICAL RE

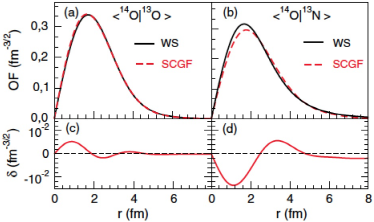

FIG. 3 (color online). Radial dependence of (a), (b) the OFs for WS and microscopic (SCGF) [30] form factors normalized to 1; (c), (d) the OF difference δ (SCGF − WS).

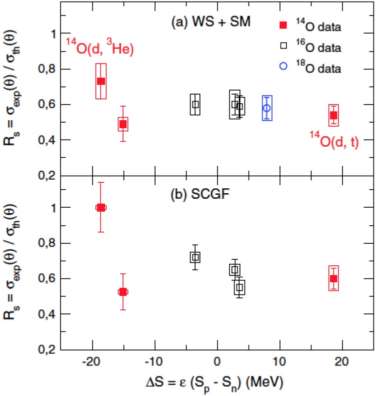

neutron & proton → transfer vs breakup

TABLE I. The normalization C^2S_{exp} for two OFs, phenomenological (WS) and microscopic (SCGF) [30]. For the WS OF, the r_0 values were chosen to reproduce $R_{\text{rms}}^{\text{HFB}}$, except for ^{16}O for which R_{rms} was taken from $(e, e'p)$ data (see text). The SFs C^2S_{th} are obtained from shell-model calculations with the WBT interaction. In the second part, the analysis was performed with microscopic OFs and SFs. The two errors for C^2S_{exp} and R_s are the experimental and analysis errors.

Reaction	E^* (MeV)	J^π	$R_{\text{rms}}^{\text{HFB}}$ (fm)	r_0 (fm)	C^2S_{exp} (WS)	C^2S_{th} $0p+2\hbar\omega$	R_s (WS)	C^2S_{exp} (SCGF)	C^2S_{th} (SCGF)	R_s (SCGF)
^{14}O (d, t) ^{13}O	0.00	$3/2^-$	2.69	1.40	1.69 (17)(20)	3.15	0.54(5)(6)	1.89(19)(22)	3.17	0.60(6)(7)
^{14}O $(d, {}^3$He$)$ ^{13}N	0.00	$1/2^-$	3.03	1.23	1.14(16)(15)	1.55	0.73(10)(10)	1.58(22)(2)	1.58	1.00(14)(1)
	3.50	$3/2^-$	2.77	1.12	0.94(19)(7)	1.90	0.49(10)(4)	1.00(20)(1)	1.90	0.53(10)(1)
^{16}O (d, t) ^{15}O	0.00	$1/2^-$	2.91	1.46	0.91(9)(8)	1.54	0.59(6)(5)	0.96(10)(7)	1.73	0.55(6)(4)
^{16}O $(d, {}^3$He$)$ ^{15}N [19,20]	0.00	$1/2^-$	2.95	1.46	0.93(9)(9)	1.54	0.60(6)(6)	1.25(12)(5)	1.74	0.72(7)(3)
	6.32	$3/2^-$	2.80	1.31	1.83(18)(24)	3.07	0.60(6)(8)	2.24(22)(10)	3.45	0.65(6)(3)
^{18}O $(d, {}^3$He$)$ ^{17}N [21]	0.00	$1/2^-$	2.91	1.46	0.92(9)(12)	1.58	0.58(6)(10)			

TABLE I: Summary of one-nucleon knockout results from ^{14}O at 53 MeV/nucleon. The calculated inclusive cross sections σ_{TC} from the transfer-to-the-continuum approach are shown and compared to the measured (σ_{exp}) cross sections. Theoretical spectroscopic factors C^2S are calculated with the WBT interaction [?]. Reduction factors are indicated and defined as R_f in order to distinguish from the strong absorption radius notation (R_s).

Res.	E (MeV)	J^π	σ_{exp} (mb)	C^2S	σ_{sp} (mb)	$\sigma_{sp}(no_p)$ (mb)	σ_{TC} (mb)	$\sigma_{TC}(no_p)$ (mb)	R_f
^{13}N	0.0	$1/2^-$	58(4)	1.83	34.18		53		0.91
^{13}O	0.0	$3/2^-$	14(1)	3.15	10.94	8.6	34.47	27.1	0.52

Conclusions

- "Good" observables from breakup reactions identified: core parallel momentum distributions and absolute cross sections.

Conclusions

- "Good" observables from breakup reactions identified: core parallel momentum distributions and absolute cross sections.
- Dynamics reasonably well understood.

Conclusions

- "Good" observables from breakup reactions identified: core parallel momentum distributions and absolute cross sections.
- Dynamics reasonably well understood.
- Rôle of structure clarified.

Conclusions

- "Good" observables from breakup reactions identified: core parallel momentum distributions and absolute cross sections.
- Dynamics reasonably well understood.
- Rôle of structure clarified.
- Transfer and knockout seem to give consistent results after all and reduction factors of spectroscopic factors are within known limits from (e,e') on normal nuclei.

Conclusions

- "Good" observables from breakup reactions identified: core parallel momentum distributions and absolute cross sections.
- Dynamics reasonably well understood.
- Rôle of structure clarified.
- Transfer and knockout seem to give consistent results after all and reduction factors of spectroscopic factors are within known limits from (e,e') on normal nuclei.
- Re-writing Nuclear Physics textbooks: 30 years with RIBs.

Conclusions

- "Good" observables from breakup reactions identified: core parallel momentum distributions and absolute cross sections.
- Dynamics reasonably well understood.
- Rôle of structure clarified.
- Transfer and knockout seem to give consistent results after all and reduction factors of spectroscopic factors are within known limits from (e,e') on normal nuclei.
- Re-writing Nuclear Physics textbooks: 30 years with RIBs.

- This talk is in memory of Nicole Vinh Mau with whom I started to work on exotic nuclei and from whom I learned a lot about physics, life and the joys of both.